Scaling of self-stimulated spin echoes

Downloaded from: https://research.chalmers.se, 2024-03-20 12:23 UTC

Citation for the original published paper (version of record):
de Graaf, S., Jayaraman, A., Kubatkin, S. et al (2024). Scaling of self-stimulated spin echoes. Applied Physics Letters, 124(2). http://dx.doi.org/10.1063/5.0176953

N.B. When citing this work, cite the original published paper.

research.chalmers.se offers the possibility of retrieving research publications produced at Chalmers University of Technology.
It covers all kind of research output: articles, dissertations, conference papers, reports etc. since 2004.
research.chalmers.se is administrated and maintained by Chalmers Library

(article starts on next page)

RESEARCH ARTICLE | JANUARY 08 2024

Scaling of self-stimulated spin echoes

S. E. de Graaf ; A. Jayaraman ; S. E. Kubatkin ; A. V. Danilov ; V. Ranjan

Check for updates

Appl. Phys. Lett. 124, 024001 (2024)
https://doi.org/10.1063/5.0176953

View Online
Export Citation
CrossMark

19 January 2024 08:17:41

AIP Publishing

APL Electronic Devices
CALL FOR APPLICANTS
Seeking Editor-in-Chief
AIP Publishing

Applied Physics Letters ARTICLE pubs.aip.org/aip/apl

Scaling of self-stimulated spin echoes

Cite as: Appl. Phys. Lett. **124**, 024001 (2024); doi: 10.1063/5.0176953
Submitted: 18 September 2023 · Accepted: 29 November 2023 ·
Published Online: 8 January 2024

View Online Export Citation CrossMark

S. E. de Graaf,[1,a)] A. Jayaraman,[2] S. E. Kubatkin,[2] A. V. Danilov,[2] and V. Ranjan[1,a),b)]

AFFILIATIONS

[1] National Physical Laboratory, Teddington TW11 0LW, United Kingdom
[2] Department of Microtechnology and Nanoscience MC2, Chalmers University of Technology, SE-41296 Goteborg, Sweden

[a)] **Authors to whom correspondence should be addressed:** sdg@npl.co.uk; vranjan@tifrh.res.in
[b)] **Present address:** Tata Institute of Fundamental Research Hyderabad, Gopanpally, Hyderabad 500046, Telangana, India.

ABSTRACT

Self-stimulated echoes have recently been reported in the high cooperativity and inhomogeneous coupling regime of spin ensembles with superconducting resonators. In this work, we study their relative amplitudes using echo-silencing made possible by a fast frequency tunable resonator. The highly anisotropic spin linewidth of Er^{3+} electron spins in the $CaWO_4$ crystal also allows to study the dependence on spin-resonator ensemble cooperativity. It is demonstrated that self-stimulated echoes primarily result from a combination of two large control pulses and the echo preceding it.

© 2023 Author(s). All article content, except where otherwise noted, is licensed under a Creative Commons Attribution (CC BY) license (*http://creativecommons.org/licenses/by/4.0/*). https://doi.org/10.1063/5.0176953

19 January 2024 08:17:41

In conventional magnetic resonance spectroscopy, stimulated echoes (STE) are known to occur when more than two control pulses are applied to spins. Stimulated echoes refocus the polarization grating stored on the longitudinal axis,[1] in contrast to Hahn echoes, which refocus the coherence generated on the transverse axes. In specific cases, Hahn echo emissions into the cavity can themselves induce further evolution of the spins. Such back action is commonly referred to as radiation damping in nuclear magnetic resonance.[2,3] So-called self-stimulated echoes (SSEs) are a direct consequence of strong back action, resulting in the emitted echo to stimulate another echo emission. Although first observed in 1954,[4] SSEs have recently received renewed attention.[5–7] This is because applications, such as high sensitivity electron spin resonance spectroscopy[8–12] and microwave quantum memories,[13–18] make use of spin ensembles strongly coupled to superconducting resonators,[19–30] a regime where SSEs are prevalent.

The ensemble coupling of spins with a common resonator mode is quantified by the cooperativity $C = 4g_{\mathrm{ens}}^2/\Gamma\kappa$, where $g_{\mathrm{ens}} = g_0\sqrt{N}$, g_0 the single spin-photon coupling strength, Γ the inhomogeneous spin linewidth, κ the total loss rate of the resonator, and N the number of spins. When $C \ll 1$, emitted echo fields are dissipated from the resonator before they could interact with the spin ensemble again. On the other hand, when $C \gg 1$, a strong collective feedback effect of the emitted field on the spins, e.g., super-radiance[31] and radiation damping,[2] can dominate the spin-dynamics. The intermediate regime of optimal impedance matching $C = 1$ is especially relevant for maximum efficiency quantum memories.[32] It is the purpose of this paper to experimentally study the scaling of self-stimulated echoes in these different regimes. Our study is, in particular, aided by the use of a fast frequency tunable superconducting resonator[33] for controlled emission of radiation into the resonator.[34] Although our results are presented using conventions of spin ensemble based microwave quantum memories,[13,32] these are readily applicable to a wider range of experiments of inhomogeneous broadened two-level systems coupled to microwave and optical cavities, such as room temperature microwave amplification,[35,36] mode cooling,[37,38] and optical quantum memories and transduction.[39,40]

Generation of SSEs can be understood using a simplified phase evolution in time, as proposed in Ref. 5 and schematically presented in Fig. 1(a). When strong inhomogeneities of Rabi angles of spins exist, a control pulse brings the spins to different points on the Bloch sphere, which for simplicity can be decomposed into a subset of ground state (g) and excited state (e) amplitudes. A second control pulse at a time τ bifurcates the previous spin amplitudes into four subsets causing a refocusing at the time 2τ between two evolution trajectories, i.e., a conventional two-pulse Hahn echo. The emitted Hahn echo then itself acts like a pulse on spins such that new branches of spin evolution appear and additional refocusing events occur at a time 3τ. Subsequent echoes create more bifurcations and more refocusing events separated by τ.

We start our experimental studies by qualitatively verifying the sketch of Fig. 1(a), which, in particular, illustrates that formation of SSEs requires phase evolution from all the pulses and echoes preceding it.

© Author(s) 2023

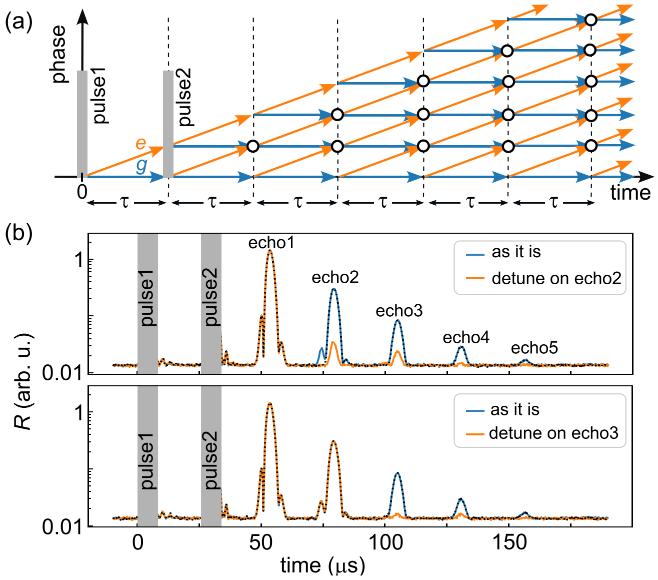

FIG. 1. Self-stimulated spin echoes (SSE). (a) A schematic of refocusing mechanism leading to self-stimulated echoes at 3τ, 4τ, 5τ,… as originally described in Ref. 5. (b) Measured magnitude of echo trains using two pulses of same amplitude, duration $2\,\mu$s, and phase, and $\tau = 25\,\mu$s. Two panels compare cases when the resonator is detuned to selectively suppress echo2 (top) or echo3 (bottom) emissions. Dashed curves in top (bottom) panels correspond to cases when the same resonator detuning pulse is applied between echo1 (echo2) and echo2 (echo3). Note that the dashed lines lie almost entirely on top of the solid lines, i.e., detuning in-between echoes has no effect. Measurements are done at $C = 3$.

Echo trains measured using two control pulses of the same amplitude and phase are shown in Fig. 1(b). Note that the magnitude is plotted in the logarithmic scale. We observe that all subsequent echoes are suppressed when we detune the resonator frequency by an amount $\Delta\omega \gg \kappa$ to suppress the emission of echo2 (top panel).[34] Applying the same duration detuning pulses between the echoes (dashed curves) produces no change thus proving that the detuning pulses do not generate significant phase noise to cause a suppression of echoes. The same observation of subsequent echo suppression is made when echo3 (bottom panel) is silenced. These suggest that contribution of two-pulse refocusing to SSE, e.g., from pulse1 and echo1 in echo3, is small. In the following, we expand on the preceding observations and semi-quantitatively study the relative amplitudes of SSEs using *in situ* control of radiation fields in the resonator and spin-resonator cooperativity.

Our electron spins (with effective $S = 1/2$) are provided by bulk doped Er^{3+} substitutional ions in a $\mathrm{CaWO_4}$ crystal with a nominal concentration of 50 ppm. The crystal is held with vacuum grease on a superconducting resonator of frequency $\omega_0/2\pi = 6.5$ GHz operating in the overcoupled regime with a loss rate of $\kappa_c/2\pi = 1.9 \pm 0.1$ MHz. The bulk distribution of Er^{3+} and narrow inductor width of $1\,\mu$m naturally result in extremely inhomogeneous tipping angles bringing spins to different points on the Bloch sphere after a control pulse. Two additional properties are relevant to this study. First, the kinetic inductance of the superconducting resonators (film thickness = 50 nm and inductor width = $1\,\mu$m) made from NbN allows the resonance frequency to be rapidly tuned by passing a bias current through the inductor strip of the resonator.[33] Second, it is possible to access different cooperativity C in the same setup. This is because two isotopes of Er^{3+}, one without a nuclear spin $I = 0$ (77%) and the rest with $I = 7/2$ (Ref. 41) couple with different numbers of spins at different transitions. Moreover, fine tuning of C is facilitated by the spin linewidth varying with the direction of the applied magnetic field (angle ϕ with c-axis) as the highly anisotropic gyromagnetic tensor ($\gamma_{ab} = 117$ MHz/mT and $\gamma_c = 17$ MHz/mT)[42] responds to the charge noise from crystal defects.[43,44] We note that variation in $g_{\rm ens}$ with ϕ is relatively small due to bulk implantation of Er^{3+} and strongly inhomogeneous B_1 field around the inductor. The crystal is placed such that the inductor is parallel to the c-axis. The experiments are performed at the base temperature of a dilution refrigerator at 20 mK, with the magnetic field aligned with the c-axis ($\phi \sim 0$) unless mentioned explicitly. More details of the experimental setup can be found in Ref. 34.

The resonator tunability helps to control the back action of the echo field on the spins, that is to vary spin rotations during the echo emission, and study the amplitudes of subsequent SSE. As shown in the sketch of Fig. 2(a), two pulses of the same amplitude and phase are applied and the resonator detuned for $20\,\mu s$, a time longer than the echo duration, with varying $\Delta\omega$ around echo1. Figure 2(b) shows the corresponding echo train traces acquired at a large demodulation bandwidth of 100 MHz to account for the relatively large total loss rate of $\kappa_{\rm tot}/2\pi \sim 7$ MHz near the $I = 0$ transition with $C = 3$ (see further below). The variation of echo1 magnitude vs normalized resonator detuning $-\Delta\omega/\kappa_{\rm tot}$ is plotted in Fig. 2(c), and the observed decay is well accounted for by the resonator filtering function $(\kappa_{\rm tot}/2)/\sqrt{\Delta\omega^2 + \kappa_{\rm tot}^2/4}$.[34] Similar to Fig. 1(b), subsequent echoes, echo2 and echo3, are progressively suppressed. To quantify their relative suppression, we plot the amplitude of echo2 and echo3 as a function of echo1 and echo2, respectively, in Fig. 2(d). A linear dependence (proportionality constant 0.16 and 0.12, respectively) describes the echo2 and echo3 data well.

Full quantitative understanding of the scaling of SSE is challenging due to the lack of knowledge of exact spin frequency detuning and coupling strength distribution. Here, we use a minimalist model to explain the scaling of echo2 and echo3 using the classical Bloch theory. Three pulses with arbitrary flip angles β_i produce a STE with an amplitude proportional to $\sin(\beta_1)\sin(\beta_2)\sin(\beta_3)$,[1] where we assume pulse delay $\tau \ll T_2$, T_1. Using control pulses of the same Rabi angle β and the fact that resulting echo1 fields are relatively much smaller, the resulting spin rotation from back action is $\sin(\theta_1) \approx \theta_1$. Then, the STE contribution of echo2 is equal to $\theta_1 \sin^2(\beta)$, where θ_i denotes the much smaller rotation angle from echo back action. Similarly, the two-pulse Hahn echo contribution of echo2 (from pulse2 and echo1) is proportional to $\theta_1^2 \sin(\beta)$. The latter is smaller in magnitude than the STE contribution as long as $\beta \gg \theta_1$. Thus, linear scaling of echo2 with echo1 can be established. Similar arguments can be made for echo3 to show that the dominating contribution comes from a three-pulse STE from pulse1, pulse2, and echo2, with a resulting echo3 proportional to $\theta_2 \sin^2(\beta)$. The proportionality constant extracted from slopes in two cases is found to be similar, 0.16 and 0.12, as expected from the model.

Overall, our observations in Fig. 2(d) suggest that a SSE primarily consists of a three-pulse STE from two large control pulses and the weak echo field preceding it. Barring common prefactors, we can, thus, quantify the magnitude of the $(i+1)^{\rm th}$ echo in the limit of $\tau \ll T_1$, T_2 as

$$A_{\rm echo}^{i+1} \equiv \eta A_{\rm echo}^{i} \sin(\beta_1)\sin(\beta_2), \tag{1}$$

19 January 2024 08:17:41

© Author(s) 2023

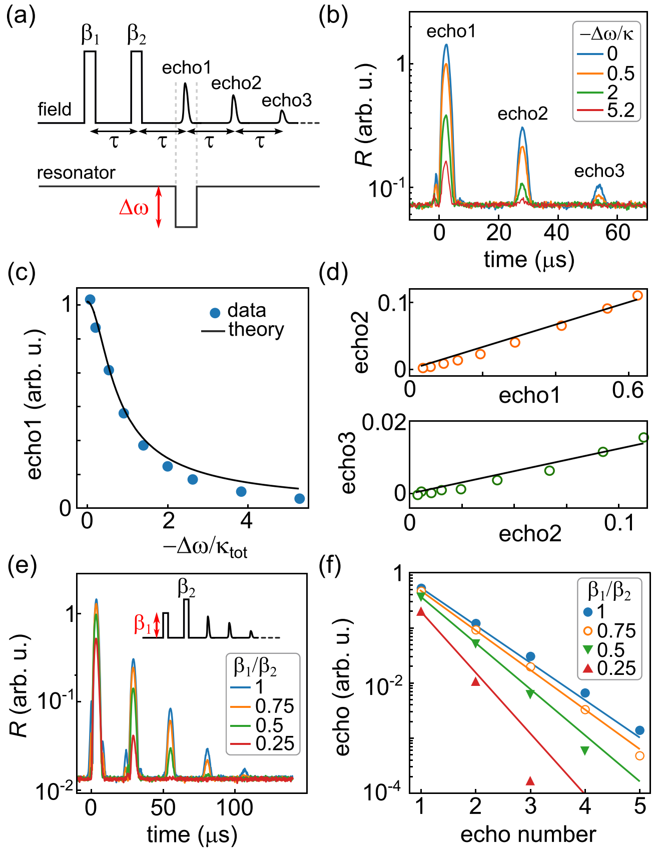

FIG. 2. SSE response vs intra-cavity field. (a) An experimental sequence consisting of two control pulses of flip angles β_i, and duration of 2 μs with a 20 μs long resonator detuning pulse across echo1 of varying $\Delta\omega$. (b) SSE traces at different $\Delta\omega$ and same flip angles $\beta = \beta_1 = \beta_2$. Larger noise floor is because of the larger measurement bandwidth $BW \sim 100$ MHz compared to other plots acquired at BW of 2 MHz. (c) Measured (symbols) and theoretical (curve) echo amplitude against different resonator detunings. (d) Scaling of echo{2, 3} amplitudes (measured: symbols and fits: lines) with corresponding changes in echo{1,2}. (e) SSE traces for different flip angles β_1 of the first control pulse and fixed β_2. The sequence is shown in the inset. (f) SSE magnitude decay for different β_1 vs echo number. Solid lines are calculated from Eq. (1). For all plots $C = 3$.

where $i > 0$ is a positive integer, and a scaling factor η^2 captures the fraction of power transferred to spins during the formation of an echo. To verify this equation further, we acquired SSE traces by varying the flip angle of the first control pulse β_1 [Fig. 2(e)], while keeping β_2 fixed. Their decay is plotted in Fig. 2(f). It has been previously shown that for strongly inhomogeneous Rabi angles in spin systems coupled to small mode volume resonators, spins for which pulse amplitudes amount to $\pi/2$ and π contribute maximum to the Hahn echo.[44–46] This allows us to set $\beta_2 = 90°$ and proportionally vary β_1 using the ratio of pulse amplitudes β_2/β_1. The SSE decays calculated from Eq. (1) are plotted as solid lines in Fig. 2(f) and show an excellent agreement with measurements using the same scaling parameter $\eta = 0.21$ across the entire dataset. Moreover, $\eta\sin^2(\beta) \approx 0.21$ is close to the measured slope in Fig. 2(d) acquired under the same experimental conditions.

We now study the dependence of SSE amplitudes on spin ensemble-resonator cooperativity. To this end, we identify two transitions in the spectrum [Fig. 3(a)] belonging to nuclear spin isotopes $I = 0$ and $I = 7/2$ ($m_I = 7/2$ is the nuclear spin projection on the magnetic field axis). From fits performed to $\kappa_{\rm tot} = \kappa + g_{\rm ens}^2\Gamma/(\Delta\omega_s^2 + \Gamma^2/4)$,[21] we find coupling strengths $g_{\rm ens}/2\pi = 10 \pm 1$ and 1.2 ± 0.1 MHz, and spin linewidths $\Gamma/2\pi = 76 \pm 5$ and 15 ± 1 MHz, and corresponding cooperativity $C = 3$ and 0.2, respectively. Here $\Delta\omega_s$ is the magnetic field dependent detuning of the spin transition frequency from the resonator. The difference in number of spins is consistent with the isotope and seven sub-level ground state populations in the $I = 7/2$ manifold. Echo response measured using the same control pulses (2 μs in duration, such that pulse bandwidth $\ll \Gamma$) at two transitions [Fig. 3(b)] shows strongly suppressed or absent SSE for the case of $C \ll 1$ and supports similar observations made in Ref. 6.

To investigate differences of spin dynamics between two Er isotopes, the spin-relaxation time is measured using an inversion recovery sequence [Fig. 3(c)]. For $I = 7/2$, we observe an exponential recovery

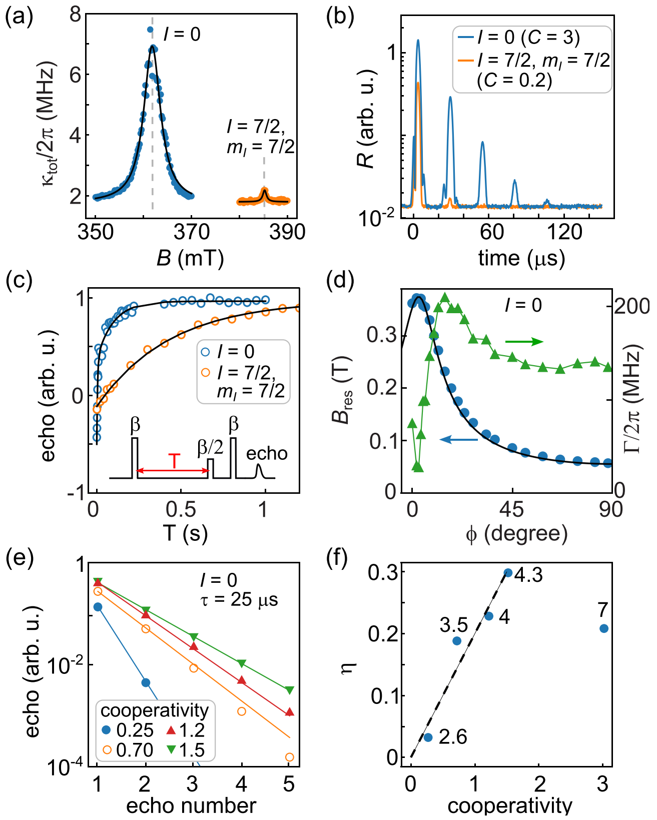

FIG. 3. SSE response vs spin-resonator cooperativity. (a) Continuous wave spectroscopy near two Er^{3+} transitions $I = 0$ and $I = 7/2$, $m_I = 7/2$ at zero angle (measured: symbols, and fit: lines). (b) Spin energy relaxation (measured: symbols, and fit: lines) using inversion recovery sequences for the two transitions at zero angle. (c) Echo response using the control pulses with the same power. (d) Spin resonance position (left axis, measured: symbols, and theory: line) and spin linewidth (right axis) for the $I = 0$ transition extracted from continuous wave spectroscopy. The magnetic field angle ϕ is relative to the c-axis of $\mathrm{CaWO_4}$. (e) Decay of SSE magnitudes for different cooperativity, but similar $\kappa_{\rm tot}$, obtained at different ϕ for the $I = 0$ transition. Solid lines are calculated using Eq. (1). (f) scaling of the extracted scaling parameter η as a function of C. Numbers next to data points are corresponding $\kappa_{\rm tot}/2\pi$ in MHz. Dashed line is a guide to the eye.

19 January 2024 08:17:41

© Author(s) 2023

with a decay constant $T_1 = 440 \pm 11\,\text{ms}$, a value consistent with a direct-phonon process.[34,47] In contrast, we observe a bi-exponential recovery for $I = 0$, with decay constants $T_1^{\text{fast}} = 4.7 \pm 0.6\,\text{ms}$ and $T_1^{\text{slow}} = 97 \pm 12\,\text{ms}$. Neither value is compatible with a direct-phonon process (scaling as $1/B^5$) or Purcell relaxation time $\kappa/4g_0^2 \approx 8\,\text{s}$ (estimated $g_0/2\pi < 100\,\text{Hz}$ for our resonator geometry). More studies are needed to fully understand the behavior of T_1 across the two transitions. The role of incoherent radiation from enhanced spin relaxation toward formation of SSEs can, however, be ruled out as resonator detuning pulses of duration $20\,\mu\text{s}$ applied in-between the echoes [dashed curves in Fig. 1(b)] do not alter the subsequent echoes. We also measure spin coherence times T_2 at two transitions and find the contrasting SSE amplitudes to not be related to the relative T_2 times. In fact, $T_2 = 2.5\,\text{ms}$ for $I = 7/2$ is four times longer compared to that for $I = 0$ and possibly limited by instantaneous diffusion.[48,49]

Another control of cooperativity is achieved by different Γ of the spin ensemble obtained when rotating the applied magnetic field with respect to the *c*-axis of the crystal. Figure 3(d) shows measured magnetic field B_{res} at which the $I = 0$ transition is resonant with the resonator (left axis) and the extracted spin linewidth Γ (right axis). The B_{res} positions agree with the spin Hamiltonian of Er^{3+} with a reasonable misalignment angle of 2.5° from the true *c*-axis. We observed a change in $\Gamma/2\pi$ from 30 MHz at $\phi = 2.5°$ to 210 MHz at $\phi = 21°$. Similar observations have been made previously[43,44] and attributed to a combination of local electric fields from charge defects, charge compensation, and lack of inversion symmetry at the substitutional Ca^{2+} sites. On the other hand, the extracted ensemble coupling strength g_{ens} decreases by only 10% in this ϕ range. The small variation in g_{ens} is consistent with g_0 calculated from the anisotropic gyromagnetic tensor, inhomogeneous B_1 field around the inductor of the resonator, and bulk distribution of Er^{3+} in the crystal.[47]

For SSE measurements, we choose slightly off-resonant B fields at different ϕ to achieve a maximum echo amplitude.[49] The SSE magnitudes measured with the same control pulses and delay $\tau = 25\,\mu\text{s}$ are plotted as a function of echo number in Fig. 3(e) for different cooperativity C. We note that the off-resonant C is extracted by comparing the intra-cavity field measured at a repetition rate $\gamma_{\text{rep}} \ll T_1$ (spins saturated) with that taken at $\gamma_{\text{rep}} \gg T_1$ (spins polarized).[15,17] For all values of C, we observe an exponential decay of echo amplitudes, similar to Fig. 2(e) and Ref. 6. For extracting η using Eq. (1), once again we set $\beta_{1,2} = 90°$ to select the spins that maximally contribute to SSE amplitudes. The calculated SSE decays and corresponding η for different C are plotted in Figs. 3(e) and 3(f). Interestingly, for small C, the scaling parameter η increases in an apparent linear fashion with C. However, η for $C = 3$ deviates from the linear trend. There are two specifics important to this. First, a much larger κ_{tot} results in a smaller spin rotation during echo back action. Second, for large C or strong radiation damping, all three spin magnetization components are expected to start evolving in a highly non-linear fashion.[3] Neither of these are captured by our simple model [Eq. (1)] implying a more complex dependence of η on C.

In conclusion, we have used control of intra-cavity field, in particular through echo-silencing, and cooperativity tuning to study scaling of self-stimulated echoes in a strongly inhomogeneously coupled spin ensemble to a small mode volume superconducting resonator. Our results demonstrate that the amplitude of a self-stimulated echo primarily arises from a three pulse stimulated echo using two large control pulses and the preceding echo field. Further studies will target a larger range of C, especially at a fixed κ_{tot}, to map out the scaling and decay of SSE amplitudes against C. STE and SSE in combination with phase imprinting[34,50] could also be used to implement selective *in situ* magnetic resonance techniques such as diffusion spectroscopy and imaging.[51]

We acknowledge the support from the UK Department for Science, Innovation and Technology through the UK national quantum technologies program. S.D.G. acknowledges support by the Engineering and Physical Sciences Research Council (EPSRC) (Grant No. EP/W027526/1). The Chalmers group acknowledges the support from the Swedish Research Council (VR) (Grant Agreement Nos. 2019-05480 and 2020-04393), EU H2020 European Microkelvin Platform (Grant Agreement No. 824109), and from Knut and Alice Wallenberg Foundation via the Wallenberg Centre for Quantum Technology (WACQT). This work was performed in part at Myfab Chalmers.

AUTHOR DECLARATIONS

Conflict of Interest

The authors have no conflicts to disclose.

Author Contributions

Sebastian E. de Graaf: Conceptualization (equal); Data curation (supporting); Formal analysis (supporting); Funding acquisition (equal); Investigation (lead); Methodology (equal); Supervision (lead); Writing – original draft (equal); Writing – review & editing (equal). **Aditya Jayaraman:** Resources (equal); Writing – review & editing (supporting). **Sergey Kubatkin:** Funding acquisition (equal); Resources (supporting); Supervision (supporting); Writing – review & editing (equal). **Andrey V. Danilov:** Funding acquisition (equal); Resources (lead); Supervision (equal); Writing – review & editing (equal). **Vishal Ranjan:** Conceptualization (equal); Data curation (lead); Formal analysis (lead); Investigation (equal); Methodology (equal); Resources (equal); Writing – original draft (lead); Writing – review & editing (equal).

DATA AVAILABILITY

The data that support the findings of this study are available from the corresponding authors upon reasonable request.

REFERENCES

[1] A. Schweiger and G. Jeschke, *Principles of Pulse Electron Paramagnetic Resonance* (Oxford University Press, 2001).
[2] N. Bloembergen and R. V. Pound, Phys. Rev. **95**, 8 (1954).
[3] M. P. Augustine and E. L. Hahn, J. Chem. Phys. **107**, 3324 (1997).
[4] J. P. Gordon and K. D. Bowers, Phys. Rev. Lett. **1**, 368 (1958).
[5] K. Debnath, G. Dold, J. J. L. Morton, and K. Mølmer, Phys. Rev. Lett. **125**, 137702 (2020).
[6] S. Weichselbaumer, M. Zens, C. W. Zollitsch, M. S. Brandt, S. Rotter, R. Gross, and H. Huebl, Phys. Rev. Lett. **125**, 137701 (2020).
[7] A. Blank, B. Koren, and A. Sherman, J. Magn. Reson. Open **16–17**, 100133 (2023).
[8] A. Bienfait, J. J. Pla, Y. Kubo, M. Stern, X. Zhou, C. C. Lo, C. D. Weis, T. Schenkel, M. L. W. Thewalt, D. Vion, D. Esteve, B. Julsgaard, K. Mølmer, J. J. L. Morton, and P. Bertet, Nat. Nanotechnol. **11**, 253 (2016).
[9] C. Eichler, A. J. Sigillito, S. A. Lyon, and J. R. Petta, Phys. Rev. Lett. **118**, 037701 (2017).

19 January 2024 08:17:41

© Author(s) 2023

[10] S. Probst, A. Bienfait, P. Campagne-Ibarcq, J. J. Pla, B. Albanese, J. F. Da Silva Barbosa, T. Schenkel, D. Vion, D. Esteve, K. Mølmer, J. J. L. Morton, R. Heeres, and P. Bertet, Appl. Phys. Lett. **111**, 202604 (2017).

[11] V. Ranjan, S. Probst, B. Albanese, T. Schenkel, D. Vion, D. Esteve, J. J. L. Morton, and P. Bertet, Appl. Phys. Lett. **116**, 184002 (2020).

[12] R. P. Budoyo, K. Kakuyanagi, H. Toida, Y. Matsuzaki, and S. Saito, Appl. Phys. Lett. **116**, 194001 (2020).

[13] B. Julsgaard, C. Grezes, P. Bertet, and K. Mølmer, Phys. Rev. Lett. **110**, 250503 (2013).

[14] J. J. L. Morton and P. Bertet, J. Magn. Reson. **287**, 128 (2018).

[15] C. Grezes, B. Julsgaard, Y. Kubo, M. Stern, T. Umeda, J. Isoya, H. Sumiya, H. Abe, S. Onoda, T. Ohshima, V. Jacques, J. Esteve, D. Vion, D. Esteve, K. Mølmer, and P. Bertet, Phys. Rev. X **4**, 021049 (2014).

[16] S. Probst, H. Rotzinger, A. V. Ustinov, and P. A. Bushev, Phys. Rev. B **92**, 014421 (2015).

[17] V. Ranjan, J. O'Sullivan, E. Albertinale, B. Albanese, T. Chanelière, T. Schenkel, D. Vion, D. Esteve, E. Flurin, J. J. L. Morton, and P. Bertet, Phys. Rev. Lett. **125**, 210505 (2020).

[18] J. O'Sullivan, O. W. Kennedy, K. Debnath, J. Alexander, C. W. Zollitsch, M. Šimėnas, A. Hashim, C. N. Thomas, S. Withington, I. Siddiqi, K. Mølmer, and J. J. L. Morton, Phys. Rev. X **12**, 041014 (2022).

[19] A. Imamoglu, Phys. Rev. Lett. **102**, 083602 (2009).

[20] Y. Kubo, F. R. Ong, P. Bertet, D. Vion, V. Jacques, D. Zheng, A. Dréau, J.-F. Roch, A. Auffeves, F. Jelezko, J. Wrachtrup, M. F. Barthe, P. Bergonzo, and D. Esteve, Phys. Rev. Lett. **105**, 140502 (2010).

[21] D. I. Schuster, A. P. Sears, E. Ginossar, L. DiCarlo, L. Frunzio, J. J. L. Morton, H. Wu, G. A. D. Briggs, B. B. Buckley, D. D. Awschalom, and R. J. Schoelkopf, Phys. Rev. Lett. **105**, 140501 (2010).

[22] E. Abe, H. Wu, A. Ardavan, and J. J. L. Morton, Appl. Phys. Lett. **98**, 251108 (2011).

[23] X. Zhu, S. Saito, A. Kemp, K. Kakuyanagi, S.-I. Karimoto, H. Nakano, W. J. Munro, Y. Tokura, M. S. Everitt, K. Nemoto, M. Kasu, N. Mizuochi, and K. Semba, Nature **478**, 221 (2011).

[24] R. Amsüss, C. Koller, T. Nöbauer, S. Putz, S. Rotter, K. Sandner, S. Schneider, M. Schramböck, G. Steinhauser, H. Ritsch, J. Schmiedmayer, and J. Majer, Phys. Rev. Lett. **107**, 060502 (2011).

[25] V. Ranjan, G. de Lange, R. Schutjens, T. Debelhoir, J. P. Groen, D. Szombati, D. J. Thoen, T. M. Klapwijk, R. Hanson, and L. DiCarlo, Phys. Rev. Lett. **110**, 067004 (2013).

[26] S. Probst, H. Rotzinger, S. Wünsch, P. Jung, M. Jerger, M. Siegel, A. V. Ustinov, and P. A. Bushev, Phys. Rev. Lett. **110**, 157001 (2013).

[27] H. Huebl, C. W. Zollitsch, J. Lotze, F. Hocke, M. Greifenstein, A. Marx, R. Gross, and S. T. B. Goennenwein, Phys. Rev. Lett. **111**, 127003 (2013).

[28] A. J. Sigillito, H. Malissa, A. M. Tyryshkin, H. Riemann, N. V. Abrosimov, P. Becker, H.-J. Pohl, M. L. W. Thewalt, K. M. Itoh, J. J. L. Morton, A. A. Houck, D. I. Schuster, and S. A. Lyon, Appl. Phys. Lett. **104**, 222407 (2014).

[29] B. C. Rose, A. M. Tyryshkin, H. Riemann, N. V. Abrosimov, P. Becker, H.-J. Pohl, M. L. W. Thewalt, K. M. Itoh, and S. A. Lyon, Phys. Rev. X **7**, 031002 (2017).

[30] J. R. Ball, Y. Yamashiro, H. Sumiya, S. Onoda, T. Ohshima, J. Isoya, D. Konstantinov, and Y. Kubo, Appl. Phys. Lett. **112**, 204102 (2018).

[31] R. H. Dicke, Phys. Rev. **93**, 99 (1954).

[32] M. Afzelius, N. Sangouard, G. Johansson, M. U. Staudt, and C. M. Wilson, New J. Phys. **15**, 065008 (2013).

[33] S. Mahashabde, E. Otto, D. Montemurro, S. de Graaf, S. Kubatkin, and A. Danilov, Phys. Rev. Appl. **14**, 044040 (2020).

[34] V. Ranjan, Y. Wen, A. K. V. Keyser, S. E. Kubatkin, A. V. Danilov, T. Lindström, P. Bertet, and S. E. de Graaf, Phys. Rev. Lett. **129**, 180504 (2022).

[35] M. Oxborrow, J. D. Breeze, and N. M. Alford, Nature **488**(7411), 353 (2012).

[36] A. Sherman, O. Zgadzai, B. Koren, I. Peretz, E. Laster, and A. Blank, Sci. Adv. **8**, eade6527 (2022).

[37] W. Ng, H. Wu, and M. Oxborrow, Appl. Phys. Lett. **119**, 234001 (2021).

[38] D. P. Fahey, K. Jacobs, M. J. Turner, H. Choi, J. E. Hoffman, D. Englund, and M. E. Trusheim, Phys. Rev. Appl. **20**, 014033 (2023).

[39] B. Kraus, W. Tittel, N. Gisin, M. Nilsson, S. Kröll, and J. I. Cirac, Phys. Rev. A **73**, 020302 (2006).

[40] A. I. Lvovsky, B. C. Sanders, and W. Tittel, Nat. Photonics **3**, 706 (2009).

[41] J. V. Rakonjac, Y.-H. Chen, S. P. Horvath, and J. J. Longdell, Phys. Rev. B **101**, 184430 (2020).

[42] B. G. Enrique, J. Chem. Phys. **55**, 2538 (1971).

[43] W. B. Mims and R. Gillen, Phys. Rev. **148**, 438 (1966).

[44] M. L. Dantec, M. Rančić, S. Lin, E. Billaud, V. Ranjan, D. Flanigan, S. Bertaina, T. Chanelière, P. Goldner, A. Erb, R. B. Liu, D. Estève, D. Vion, E. Flurin, and P. Bertet, Sci. Adv. **7**, eabj9786 (2021).

[45] V. Ranjan, S. Probst, B. Albanese, A. Doll, O. Jacquot, E. Flurin, R. Heeres, D. Vion, D. Esteve, J. J. L. Morton, and P. Bertet, J. Magn. Reson. **310**, 106662 (2020).

[46] J. O'Sullivan, O. W. Kennedy, C. W. Zollitsch, M. Šimėnas, C. N. Thomas, L. V. Abdurakhimov, S. Withington, and J. J. L. Morton, Phys. Rev. Appl. **14**, 064050 (2020).

[47] M. L. Dantec, Ph.D. thesis, Université Paris-Saclay, 2022.

[48] M. Rančić, M. Le Dantec, S. Lin, S. Bertaina, T. Chanelière, D. Serrano, P. Goldner, R. B. Liu, E. Flurin, D. Estève, D. Vion, and P. Bertet, Phys. Rev. B **106**, 144412 (2022).

[49] J. Alexander, G. Dold, O. W. Kennedy, M. Šimėnas, J. O'Sullivan, C. W. Zollitsch, S. Welinski, A. Ferrier, E. Lafitte-Houssat, T. Lindström, P. Goldner, and J. J. L. Morton, Phys. Rev. B **106**, 245416 (2022).

[50] H. Wu, R. E. George, J. H. Wesenberg, K. Mølmer, D. I. Schuster, R. J. Schoelkopf, K. M. Itoh, A. Ardavan, J. J. L. Morton, and G. A. D. Briggs, Phys. Rev. Lett. **105**, 140503 (2010).

[51] D. Burstein, Concepts Magn. Reson. **8**, 269 (1996).

19 January 2024 08:17:41

© Author(s) 2023